First-principles study of H ordering in the α phase of M-H systems (M=Sc, Y, Ti, Zr)

Jorge Garcés,[1] Rafael González,[2] and Peter Vajda[3]
[1]*Centro Atómico Bariloche, Comisión Nacional de Energía Atómica, Bariloche, Río Negro, Argentina*
[2]*GEMA-Grupo de Estudio de Materiales, Universidad Nacional de Colombia, Bogotá, Colombia*
[3]*Laboratoire des Solides Irradiés, CNRS-CEA, Ecole Polytechnique, +F-91128 Palaiseau, France*
(Received 10 September 2008; revised manuscript received 21 January 2009; published 26 February 2009; publisher error corrected 19 March 2009)

The effect of local atomic relaxations on the structural stability of the peculiar quasiunidimensional H-R-H pair ordering occurring at low-temperature in a series of hexagonal rare-earth-hydrogen solid solutions, α-RH_x, (R=Sc, Y, Ho, Er, Tm, and Lu) is studied by means of density-functional theory. We are proposing here a first-principles-based model, which, by considering the relaxation of the host metal cell, yields for the first time a suitable explanation for the observed chainlike short-range ordering through a coherent stress field along the chain, as well as for its limitation to the six metals in question—a phenomenon never completely understood theoretically.

DOI: 10.1103/PhysRevB.79.054113 PACS number(s): 61.50.Ah, 71.15.−m, 81.30.Mh, 82.30.Rs

I. INTRODUCTION

The rare-earth metals (R) absorb hydrogen readily and form—depending on concentration and temperature—solid solutions (α phase) and/or hydrides (β and/or γ phases), with often wide existence ranges around the stoichiometric compositions.[1] These deviations from stoichiometry are responsible for various interesting physical phenomena such as H-sublattice ordering and metal-insulator transitions, which are visible in many structural and electronic properties. A particularly exciting characteristic is the presence of a metastable low-T solid solution α^*-RH_x phase observed in Sc, Y, Ho, Er, Tm, and Lu up to rather high x concentrations and manifest for example as anomalies in resistivity around 150 K or peaks in internal friction. Neutron-scattering experiments[2–4] have permitted to establish the α^* phase as a short-range ordered structure formed of hydrogen pairs occupying second-neighbor tetrahedral (T) sites around a metal atom along the c axis, H-R-H, and arranging into zigzagging (probably helicoidal) pairs in the c direction, the pairs being shifted along the b axis of the hcp cell forming a chainlike structure as it is shown in Fig. 1. The chain lengths varied from one system to another and seemed to correlate with the elastic anisotropy of the metal. (A review of the experimental situation has been given in Ref. 1.)

This peculiar structure has intrigued the theoreticians soon after its discovery more than 20 years ago, who had studied several specific aspects of its manifestation. Thus, it was found in total-energy calculations using cluster models,[5] supercells,[6] and self-consistent pseudopotentials[7] that the second-neighbor T-site occupation along the c axis was, indeed, the most stable for the H atoms in yttrium, while lattice-statics methods of statistical thermodynamics using empirical "electrochemical" potentials permitted to infer strain-induced ordering into one-dimensional concentration waves in Sc, Y, and Lu.[8] There exist several papers dealing with rare-earth metal or hydride systems (e.g., Ref. 9) but the first theoretical effort to study the relation between chain ordering of H in the solid solution, the relaxation of internal coordinates and the electronic properties for the hypothetical YH_x (x=1/3,2/3) compounds have been presented in Ref. 10. Nevertheless, important questions remained open without a definite answer: e.g., the solubility limit in the α^* phase varying from $x_{max}(\alpha^*)$=0.03 H/R in Ho to 0.35 H/R in Sc or the source of the chain structure stability and the problem of its limitation to the above-mentioned six rare earths only, ignoring other lanthanides as well as other H-absorbing hcp metals such as Ti or Zr. Some qualitative argumentation had been used to approach the fundamentals of the phenomenon relating the picture of charge-density waves to nesting features of the Fermi surface,[3] on one hand, or implying the formation of a coherent stress field in the host lattice,[11] on the other. However, a complete understanding of the phenomenon is still unavailable.

The chain structure forms only at temperatures below ~150–170 K. At higher T, where the H-R-H pairs continue

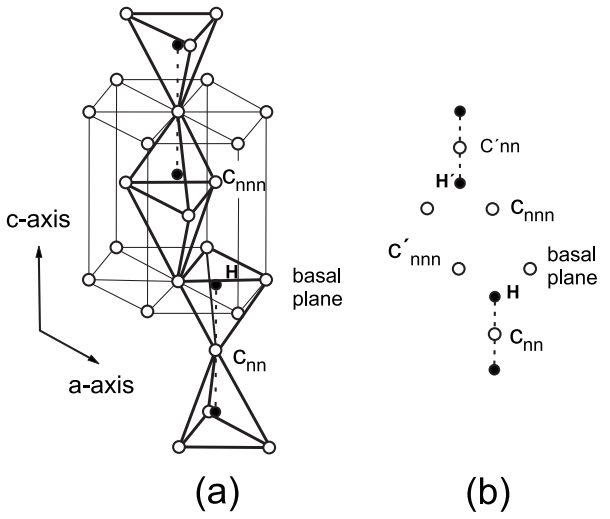

FIG. 1. (a) HCP unit cell of MH_x in the α^* phase showing two adjacent H-M-H pairs (dashed lines) shifted along the b axis. Also shown are the basal plane, the nearest (c_{nn}) and the next-nearest-neighbors (c_{nnn}) atoms to the hydrogen atom labeled H. (b) Schematic representation of the chain structure.

to be observed, vibrational effects could play an important role in the breakup of the chains. However, there is no experimental evidence regarding phonon effects upon the structural chain stability at finite temperature. In fact, Blaschko *et al.*,[12] in a phonon-dispersion study, pointed out that no influence of deuterium ordering at low temperature upon the phonon frequencies could be detected in LuD_x. Moreover, there is evidence of dynamic coupling between H-*R*-H pairs in a few alpha phase systems obtained through inelastic and quasielastic neutron scattering[13,14] (see also Ref. 1, Table 12). Therefore, a first-principles thermodynamic investigation, like that described in Ref. 15, could hide the fundamentals of this phenomenon. In the present study, on the other hand, we will look for the source of the chain stability and its exclusive occurrence in six metals through a first-principles calculation at 0 K, and we will focus our attention on the role of local atomic relaxations inside the cell assuming that they could play an essential part in the hydrogen behavior and the ensuing structural stability of the R-H systems in question. (Rare-earth elements with an incomplete 4*f* shell will not be considered in this work due to computational and code limitations for the study of noncollinear magnetism, an effect that should be included for a proper treatment of those elements.) Thus, in the present work, we shall limit our investigation to the study of the H ordering and the chain structural stability in the following complementary *M*-H systems, *M*=Sc,Y,Ti,Zr.

II. COMPUTATIONAL METHOD

The full-potential linearized augmented plane-wave (LAPW) method based on density-functional theory as it is implemented in the WIEN2K code[16] was used for the calculations. This code uses the full-potential augmented plane-wave+local orbital (APW+lo) method that makes no shape approximation to the potential or density. The generalized gradient approximation of Perdew, Burke, and Ernzerhof[17] was used for the correlation and exchange as no experimental or theoretical evidence of strong correlations was found on the systems studied here. The atomic sphere radii, R_{MT}, selected for the *M* and H elements were 2.1–2.4 bohr and 1.0–1.2 bohr, respectively. Local orbital extensions were included for the semicore states of *M* elements. The basis set size $R_{MT}K^{o}_{max}$ (R_{MT} is the smallest atomic sphere radius inside the cell and K^{o}_{max} is a cutoff for the basis function wave vector) were chosen, respectively, as 9 and 4–4.5 for pure *M* and the *M*-H systems studied. The charge-density cutoff G_{max} was selected as 75–82 $eV^{1/2}$ (in the atomic units system used by the WIEN2K package). The maximum *l* values for partial waves inside the spheres and for the non-muffin-tin matrix elements were selected to be $l_{max}=12$ and $l_{max}=6$, respectively. A mesh of 250–300 special *k* points was taken in the whole Brillouin zone. The iteration process is repeated until the calculated total energy, charge, and force components converge to less than 7×10^{-4} eV/cell, 3×10^{-4} electrons/Å^3, and 2×10^{-2} eV/Å, respectively. The minimization procedure includes the optimization as a function of the lattice parameters *a* and the *c*/*a* ratio, followed by the relaxation of the internal atomic coordinates in the optimized values of the lattice parameters. A necessary additional step includes checking for changes in the lattice parameters against atomic displacements, which could result in further minimization of the internal parameters. In our work, good agreement was found between the first and the second step in the minimization procedure. For example, the energy difference between these two steps is only 0.9 meV/cell in $ScH_{1/3}$ in the *Pmma* space group. The respective lattice-parameter changes are less than 0.1%.

III. RESULTS AND DISCUSSION

A. Exclusivity of the chain structure to six hcp elements

There is no direct theoretical information available for the *M*-H systems studied in this work (*M*=Sc,Ti,Y,Zr) related to the effects of interstitial H atoms on their local atomic environment. Hence, the first step to understand the H behavior in these hcp metals is to investigate the atomic relaxations around one H atom located in a tetrahedral site, which had been found in earlier experimental and theoretical work as being the most favorable.[1,18] For this study, a hexagonal supercell ($2\times2\times3$ hcp unit cell) in the *P*1 space group with $MH_{1/25}$ composition and the experimental lattice parameters of the pure elements have been chosen.

The theoretical results have clearly shown that there are two different relaxation patterns concerning the force components around the H atoms: (i) pattern I for Sc and Y, where the nearest-neighbor (nn) metal atoms feel small radial forces (<0.15 eV/Å) while the next-nearest-neighbor (nnn) atom along the *c* axis (c_{nnn}) feels the biggest force, similar in magnitude for the two elements (~0.5 eV/Å) and, (ii) pattern II for Ti and Zr, where all atoms feel big radial forces (>1.0 eV/Å for nn atoms), the biggest one (~1.4 eV/Å) being felt by the nearest-neighbor atom along the *c* axis (c_{nn}). In all cases, the H atom moves toward the basal plane of the tetrahedron, in agreement with experiment.[19] The $ScH_{1/25}$ and $YH_{1/25}$ relaxation pattern, also obtained for $LuH_{1/25}$ (not shown here), was confirmed by using a supercell ($3\times3\times3$ hcp unit cells) with 55 atoms in the *P*1 space group. The effect of the H atom in the $ScH_{1/55}$ supercell, for example, extends as far as 5.85 Å. The energy gain after internal coordinate relaxation is 38 meV/cell and 64 meV/cell for $ScH_{1/25}$ and $TiH_{1/25}$, respectively.

Remarkably, the chain formation is observed only in the group of elements with the first relaxation pattern, while the second group presents no isolated H pair or chain formation experimentally but only monohydride or/and dihydride phases.[18] Also, the elements belonging to the first group are those where the pair H-*R*-H was found to be the most stable configuration.[1] First-principles theoretical work confirmed this result for the Y-H system.[5–7] However, none of these theoretical papers had included the effect of local relaxations in their work. Therefore, the addition of a second H atom will allow us to evaluate the eventual role of local relaxations in the structural stability of the pairs H-*M*-H (*M*=Sc,Y;Ti,Zr) and the host-lattice reaction in the presence of two H atoms. A hexagonal supercell ($2\times2\times3$ hcp unit cell) in the *P*3*m*1 or *P*1 space group with composition $MH_{2/26}$ and the theoretical equilibrium lattice parameters are

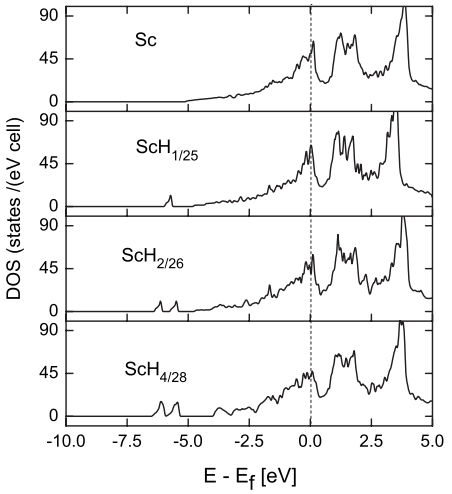

FIG. 2. Evolution of the total DOS with the composition for ScH_x ($x=0,1/25,2/26,4/28$). The figure shows the changes in the shape of the H peaks as it is the only contribution below −5 eV. The most relevant information is the change from one peak for one H atom to two peaks once the H-Sc-H pair is formed. The dashed line is the Fermi energy set to zero.

used in this study. In agreement with previous authors,[5–7] we find that the pair is the most stable configuration and that it is stabilized by local atomic relaxations in all our systems, namely Sc, Ti, Y, and Zr. The pair in the unrelaxed $ScH_{2/26}$ is more stable than two random H atoms by 77 meV/cell, while, after atomic relaxation, this difference is 86 meV/cell. The same differences in $TiH_{2/26}$ are 88 meV/cell and 39 meV/cell for the unrelaxed and relaxed situations, respectively. On the other hand, the pair is stabilized due to atomic relaxations by 72 meV/cell and 195 meV/cell in $ScH_{2/26}$ and $TiH_{2/26}$, respectively. These results show that the relaxations in $ScH_{2/26}$ stabilize the pair, while, in $TiH_{2/26}$, the stabilization is stronger in the random situation, although the energy balance still favors the pair formation.

Thus even if the force pattern for this composition shows initially the same basic features observed for all $MH_{1/25}$ cases, the behavior of the host lattice in the presence of H atoms is quite different if relaxations are included in the description. In Ti and Zr the pair is the usual one H-c_{nn}-H—symbolized by H-M-H and extends mainly to nn along the c axis. On the other hand, the influence of the H atoms on the c_{nnn} atoms in Sc and Y implies that the calculations must take them into account for a proper description of the pair and the overall relaxation behavior in these systems. As a consequence, the pair in the latter metals can be described by a linear arrangement c_{nnn}-H-c_{nnn}-H-c_{nnn} along the c axis, symbolized by M-H-M-H-M.

Although the main atomic relaxation features are very similar in each relaxation group for MH_x ($x=1/25,2/26$), there are notable changes in the hydrogen density of states (H-DOS) between both compositions. Figure 2 shows the evolution of the total DOS versus concentration for ScH_x ($x=0,1/25,2/26,4/28$). Similar results were obtained for MH_x ($M=$Ti,Y,Zr). The most relevant feature is the split of the H peak, centered around −5.5 eV for one H atom, into two peaks for each H atom for higher concentrations. In

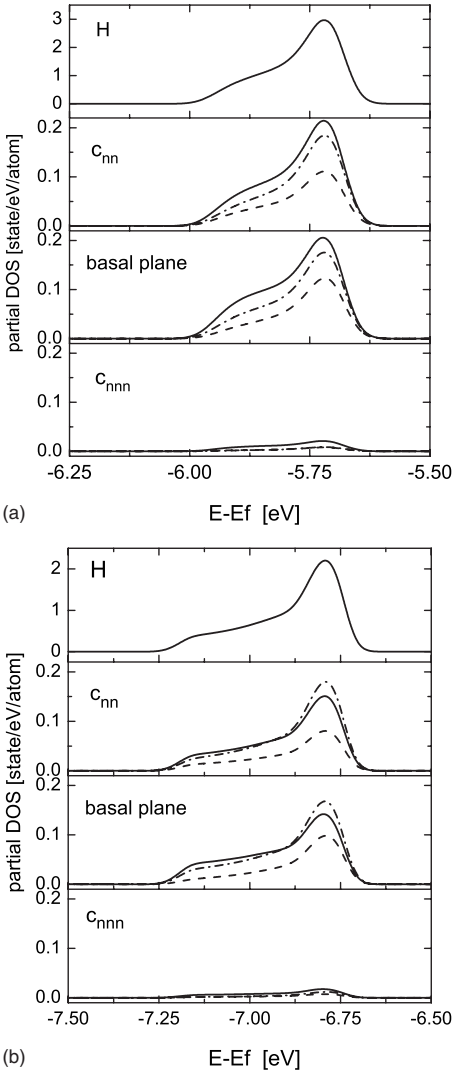

FIG. 3. Site and partial-wave analysis of the DOS for: (a) $ScH_{1/25}$ and (b) $TiH_{1/25}$. The atoms are labeled according to Fig. 1(b). s state: solid line, p state: dashed line, and d state: dot-dashed line. The bonding strength in $ScH_{1/25}$ decreases in the order s, d, and p for the c_{nn} and basal plane atomic states respectively, while in $TiH_{1/25}$ it is d, s, and p for the same atoms. A small mixing with the c_{nnn} atom orbitals is also observed.

order to analyze the atomic interaction between a hydrogen atom and its different neighbor atoms, the total DOS has been decomposed into its partial-wave (s, p, and d) components around the H, the basal plane, c_{nn} and c_{nnn} atomic sites. The analysis of the DOS around the H peak in $MH_{1/25}$ shows that the main H bonding is realized with the c_{nn} and basal plane atoms through the s, d, and p states of Sc and Y while, in Ti and Zr, the order is d, s, and p states, as shown in Figs. 3(a) and 3(b), respectively. In addition, a mixing with the c_{nnn} atom states is observed, which is smaller in Ti and Zr. The H s state has no contribution near the Fermi level. There is a drastic and unexpected change in the bonding characteristics between the H s state and the first neighbor electronic state in the structure, as shown in Fig. 4 for $ScH_{2/26}$. The higher energy peak (left side) mixes mainly with the s and d states belonging to the c_{nn} atom while the lower energy peak

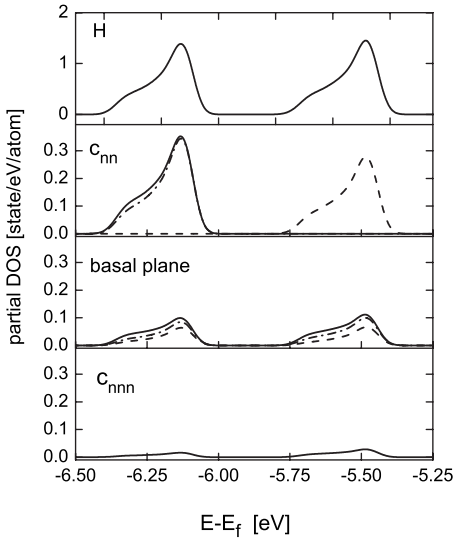

FIG. 4. Site and partial-wave analysis of the DOS for $ScH_{2/26}$. The atoms are labeled according to Fig. 1(b). *s* state: solid line, *p* state: dashed line, and *d* state: dot-dashed line. The higher energy peak (to the left) mixes mainly with the *s* and *d* states belonging to the c_{nn} atom while the lower energy peak (to the right) mixes exclusively with the c_{nn} *p* states. The basal plane and the c_{nnn} states mix equally with both peaks. Under relaxation the former does not move while the latter moves slightly, by about around 0.055 eV to higher energies.

(right side) mixes exclusively with the c_{nn} *p* states. The basal plane states mix equally with both peaks. The small mixing with the c_{nnn} states remains unchanged. Under relaxation, the former does not move while the latter moves slightly, by about 55 meV, to higher energies. This peculiar bonding structure is probably the reason for the high stability of the H-*M*-H pair observed in different structures of H with transition metals.

The previous results for the $MH_{2/26}$ systems verify the same correspondence found for the composition $MH_{1/25}$ between the behavior of each group of elements in the presence of interstitial H and the systems where the chainlike structure was observed experimentally. This correspondence poses the question about the behavior of these pairs when two of them approach each other at low temperature. For this purpose, we studied the local atomic relaxations in the system $MH_{1/7}$ with two H pairs, in a hexagonal supercell in the *Cmcm* and *P*1 space group, arranged in two different configurations: (i) two pairs *M*-H-*M*-H-*M* in the chainlike configuration [see Fig. 5(a)] and (ii) two pairs H-*M*-H as close as possible in the hcp structure (compact pairs structure) with both central metal atoms belonging to the same tetrahedron and located in two consecutive planes. The study of the local chainlike structure stability and its limitation to six metals can be reduced to the study of the competition between these two kinds of pair arrangements, which, ultimately, is the competition between the tendency to form the chainlike structure (α^* structure) or the monohydride (γ phase) and/or dihydride (δ phase).

Table I shows the effect of local atomic relaxations on the structural stability of the chain and the compact pairs structures in $MH_{1/7}$ systems (*M*=Sc, Ti, Y, and Zr). Figure 6 shows, for the same systems, the effect of local relaxations

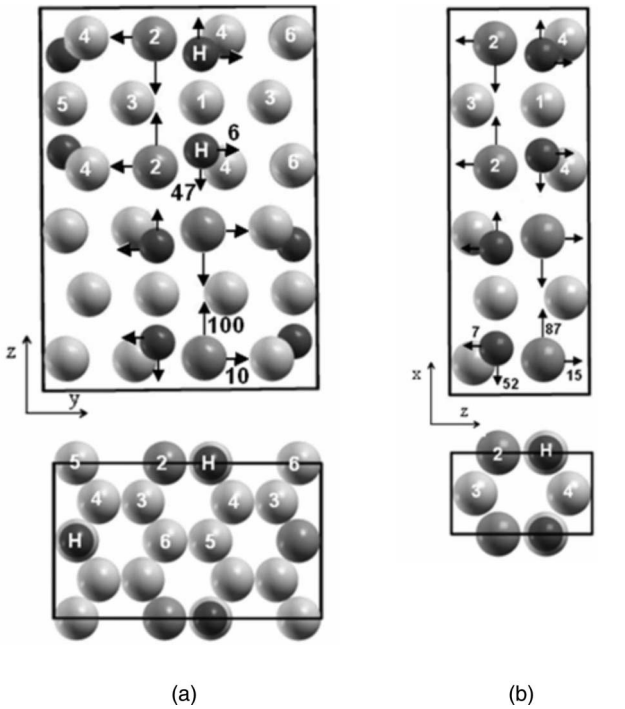

FIG. 5. Schematic view of atomic displacements (in mÅ) for the chainlike structures with compositions: (a) $ScH_{1/7}$ and (b) $ScH_{1/4}$. (The Y-H systems studied in this work present the same force components pattern for each composition.) Only displacements due to forces bigger than 4mRy/au are shown. The atoms are labeled in accordance with Table III.

on the relative stability between these two structures versus lattice parameter. Although the chain structure in $ScH_{1/7}$ ($YH_{1/7}$) is stabilized with respect to the compact pairs structure at the theoretical equilibrium lattice parameters by an amount of 37 meV/cell (58 meV/cell), a volume effect was found as the compact pairs structure becomes more stable under compression. On the other hand, the compact pairs configuration is always the most stable structure for the $TiH_{1/7}$ and $ZrH_{1/7}$ systems, and it is strongly stabilized under relaxation, in agreement with experimental results where no evidence of single pairs or chain structure were found at any temperature.[18] Thus, if local relaxations are included in the description of the *M*-H systems, the exclusive existence of

TABLE I. Effect of atomic relaxations on the structural stability of $MH_{1/7}$ systems (*M*=Sc, Ti, Y, and Zr). Energy gain differences (in meV/cell) between the relaxed and unrelaxed chainlike and compact pair structures. The total-energy calculations were made in a hexagonal supercell ($2\times2\times3$ unit hcp cell) in the *Cmcm* space group. The calculation for $ScH_{1/7}$ was made also in the *P*1 space group.

ΔE (meV/cell)	$ScH_{1/7}$	$TiH_{1/7}$	$YH_{1/7}$	$ZrH_{1/7}$
Chain	137	276	146	215
	148 (*P*1)			
Compact pairs	120	351	109	269

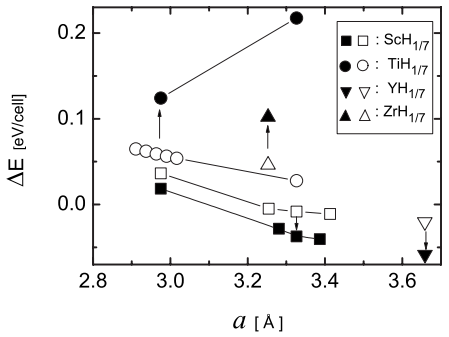

FIG. 6. Energy difference (in eV/cell) between the chainlike and compact pairs structures versus lattice parameter for: square symbol: $ScH_{1/7}$, circle: $TiH_{1/7}$; up triangle: $ZrH_{1/7}$ and down triangle: $YH_{1/7}$. Open symbols: unrelaxed structure differences; Full symbols: relaxed structure differences. The arrows are drawn at the theoretical equilibrium lattice parameter a of each system, and their directions show the effect of relaxation on the energy gain difference.

the chainlike structure to only six hcp metals can be easily explained. It would be observed only in systems with the local atomic relaxation pattern I: namely, Sc, Y, and Lu, where the atom c_{nnn} shows strongest displacement along the c axis.

B. Source of the chain structure stability

It remains to investigate the source of the chain stability in detail. For that purpose, we studied two concentrations in the chainlike structure: (i) $MH_{1/7}$ (M=Sc,Y) in the *Cmcm* space group with seven nonequivalent atoms in its basis [Fig. 5(a)] and (ii) $MH_{1/4}$ (M=Sc,Y) in the *Pmma* space group with five nonequivalent atoms in its basis [Fig. 5(b)]. The general tendencies of lattice parameters versus H contents, shown in Table II, are in good agreement with the experimental data at 300 K, when available.[1] We are able to conclude from the structural analysis that: (i) the main forces and displacements due to relaxation of internal coordinates are oriented in the c-axis direction for both compositions and are quite distinct from those obtained for the Ti-H and Zr-H systems, in agreement with the results for one and two interstitial H atoms; (ii) the H atoms approach the basal plane of their respective tetrahedron. The H displacement along the c axis is ~0.05 Å and ~0.03 Å for ScH_x and YH_x, respectively, always less than 0.1 Å in agreement with previous experimental analysis;[2] (iii) one obtains lateral displacement for all atoms due to the interaction between nearest-neighbor M-H-M-H-M pairs. The movement depends on the electronic structure of the host-lattice atom M, and the amplitudes are of the order of 0.005 Å and (0.01–0.02) Å, for H and M atoms, respectively. Figure 5 shows schematically the main displacements obtained for ScH_x (x=1/7,1/4). The same force components pattern was obtained for YH_x (x=1/7,1/4), in agreement with previous results for YH_x (x=1/3,2/3).[10] Table III shows the atomic displacements for nonequivalent atoms in the cell for compositions $MH_{1/7}$ and $MH_{1/4}$ (M=Sc,Y).

TABLE III. Atomic displacements (in mÅ) for $MH_{1/7}$ and $MH_{1/4}$ (M=Sc,Y) in the *Cmcm* space group after internal atomic coordinates relaxation for the group of atoms labeled in Fig. 5. The atom in bold shows the biggest displacement along the c axis and is the main source of the energy gain due to local atomic relaxations.

	Displacement			
Atom	$ScH_{1/7}$ (mÅ)	$YH_{1/7}$ (mÅ)	$ScH_{1/4}$ (mÅ)	$YH_{1/4}$ (mÅ)
1	18	24	23	13
2	**100**	**120**	**87**	**100**
3	7	19	2	5
4	10	24	26	30
5	22	29		
6	6	4		
H	47	34	52	33

Although it is difficult to compute with enough confidence the energy contributions due to small atomic displacements, it is possible to identify qualitatively the main source of the chain stability. The main energy gain due to relaxation is due to the displacements of the c_{nnn} and the H atoms along the c axis as was obtained previously. But, there is a small secondary energy gain (around 13–27 meV/cell) due to the atomic movements (principally due to distortion of the basal plane) produced by the interactions between pairs that can be

TABLE II. Calculated and experimental lattice parameters at 300 K (in Å) for M, $MH_{1/7}$, and $MH_{1/4}$ (M=Sc,Y) systems.

	Sc	$ScH_{1/7}$	$ScH_{1/4}$	Y	$YH_{1/7}$	$YH_{1/4}$
$a_{calc.}$ (Å)	3.314	3.326	3.338	3.651	3.659	3.691
$a_{expt.}$ (Å)	3.309[a]	3.322[b]	3.330[b]	3.648[a]	3.659[b]	3.668[c]
$c_{calc.}$ (Å)	5.170	5.239	5.301	5.696	5.755	5.832
$c_{expt.}$ (Å)	5.268[a]	5.286[b]	5.292[b]	5.732[a]	5.773[b]	5.801[c]
$c/a_{calc.}$	1.560	1.575	1.588	1.560	1.573	1.580
$c/a_{expt.}$	1.592	1.589	1.588	1.571	1.578	1.581

[a]Reference 20.
[b]Interpolated from Ref. 1.
[c]Extrapolated from Ref. 1.

TABLE IV. Energy differences (in meV/cell) between the relaxed and unrelaxed chainlike structures for $MH_{1/7}$ and $MH_{1/4}$ (M =Sc,Y). The energy gain is decomposed in two contributions: one due to the c_{nnn} and H atomic movement along the c axis, the other due to the movement of the remaining atoms belonging mainly to a tetrahedron basal plane.

ΔE (meV/cell)	$ScH_{1/7}$	$YH_{1/7}$	$ScH_{1/4}$	$YH_{1/4}$
Relaxed-unrelaxed	148	146	113	126
(c_{nnn},H)-unrelaxed	144	120	99	110
(c_{nnn},H)-relaxed	4	26	14	16

considered as the source of the chain stability. This energy gain due to interaction between nearest-neighbor pairs depends on the element and on composition, as shown in Table IV. Thus, the atom c_{nnn}, associated with each H atom and also with one of the tetrahedron basal plane of the nearest-neighbor pair (see Fig. 1), could be considered as the nexus between pairs and the responsible of the chain structure formation. It is possible that an extra energy gain is provided by the lateral interactions between chains. The short-range interaction provided through the c_{nnn} atom supports the idea of a coherent stress field along the chain suggested in Ref. 11. Its main features will depend ultimately on the different response of the electron density inside each tetrahedron due to the presence of an interstitial H atom.

Figure 7 shows the main bonding features of the chainlike structure. The small interaction between the H and c_{nnn} atoms characteristic of low concentrations, is replaced by a bonding structure reflecting the fact that the latter belongs simultaneously to the M-H-M-H-M pair and to the tetrahedron basal plane of the nearest-neighbor pair. The coupling is performed essentially with the lower energy peak while the higher energy peak mainly bonds with the nearest-neighbor states.

IV. CONCLUSIONS

The results presented in this paper suggest that local atomic relaxations are the key to understand the behavior of H atoms in the α^* phase of the R-H systems (R=Sc,Y, Ho,Er,Tm,Lu). The local relaxations around the H atoms in tetrahedral sites render plausible the R-H-R-H-R pair as well as the chainlike structure formation at low temperature and could explain the reason for the occurrence of this phenomenon in some hcp systems only. It will only occur in systems where the next-nearest neighbor to the H atom along the c axis (c_{nnn}) exhibits a movement of the order of 0.1 Å. The lateral interaction between the c_{nnn} atom and the remaining atoms located in the nearest-neighbor R-H-R-H-R pair is the principal mechanism for the H-chain formation and provides support for the existence of a coherent stress field along the chain. The DOS analysis shows that the H bonding is produced mainly with the nearest neighbors and no contribution of H s states is observed at the Fermi level.

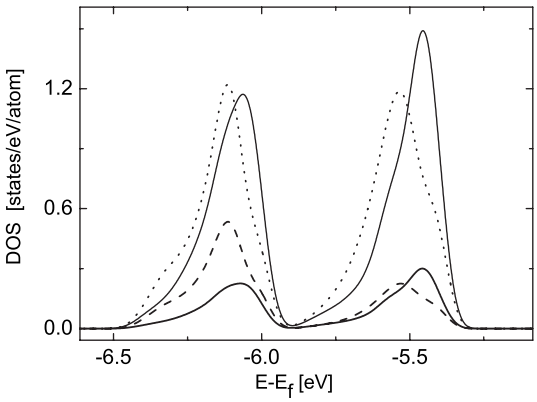

FIG. 7. Bonding features of the chainlike structure for $ScH_{1/7}$. The atoms are labeled according to Fig. 1(b). H atom: dotted line, c_{nn} atom: dashed line, H′ atom: light solid line and c_{nnn} atom: dark solid line. The figure shows the mixing of partial states belonging to different pair atoms. The figure suggests that the main bond is performed between partial states with their peak maximum located at the same energy.

ACKNOWLEDGMENTS

The authors wish to thank K. Schwarz, P. Blaha, and A. Kokalj for sharing their codes. Helpful discussions with J. Andrade Gamboa are gratefully acknowledged. This work was supported by the Agencia Nacional de Promoción Científica y Tecnológica (Argentina) through Grant No. BID/OC 12-15047.

[1] P. Vajda, *Hydrogen in Rare Earth Metals*, in Handbook on the Physics and Chemistry of Rare Earths Vol. 20, edited by K. A. Gschneidner, Jr., L. Eyring, and S. B. Marquez (North-Holland, Amsterdam, 1995), p. 207; P. Vajda, Solid State Ionics **168**, 271 (2004).
[2] O. Blaschko, G. Krexner, J. N. Daou, and P. Vajda, Phys. Rev. Lett. **55**, 2876 (1985).
[3] M. W. McKergow, D. K. Ross, J. E. Bonnet, I. S. Anderson, and O. Schaerpf, J. Phys. C **20**, 1909 (1987).
[4] I. S. Anderson, J. J. Rush, T. J. Udovic, and J. W. Rowe, Phys. Rev. Lett. **57**, 2822 (1986).
[5] F. Liu, M. Challa, S. N. Khanna, and P. Jena, Phys. Rev. Lett. **63**, 1396 (1989).
[6] C. Koudou, C. Minot, and C. Demangeat, Europhys. Lett. **13**, 263 (1990).
[7] Y. Wang and M. Y. Chou, Phys. Rev. B **49**, 13357 (1994).
[8] V. A. Tatarenko and C. L. Tsynman, Solid State Ion. **101-103**, 1061 (1997).
[9] L. G. Hector, Jr. and J. F. Herbst, J. Alloys Compd. **379**, 41 (2004).
[10] J. Garcés, J. L. Gervasoni, and P. Vajda, J. Alloys Compd. **404-406**, 126 (2005).
[11] O. Blaschko, G. Krexner, J. Pleschiutschnig, G. Ernst, J. N. Daou, and P. Vajda, Phys. Rev. B **39**, 5605 (1989).

[12] O. Blaschko, G. Krexner, L. Pintschovius, P. Vajda, and J. N. Daou, Phys. Rev. B **38**, 9612 (1988).
[13] T. J. Udovic, J. J. Rush, I. S. Anderson, and R. G. Barnes, Phys. Rev. B **41**, 3460 (1990).
[14] T. J. Udovic, J. J. Rush, N. F. Berck, and I. S. Anderson, Phys. Rev. B **45**, 12573 (1992).
[15] Y. Wang, L. G. Hector, Jr., H. Zhang, S. L. Shang, L. Q. Chen, and Z.-K. Liu, Phys. Rev. B **78**, 104113 (2008).
[16] P. Blaha, K. Schwarz, G. K. H. Madsen, D. Kvasnicka, and J. Luitz, *Wien2k, An Augmented Plane Wave + Local Orbitals Program for Calculating Crystal Properties* (Schwarz/Technische Universitat Wien, Vienna, Austria, 2001).
[17] J. P. Perdew, K. Burke, and M. Ernzerhof, Phys. Rev. Lett. **77**, 3865 (1996).
[18] Y. Fukai, *The Metal-Hydrogen System* (Springer-Verlag, Berlin, 2005).
[19] D. Khatamian, C. Stassis, and B. J. Beaudry, Phys. Rev. B **23**, 624 (1981).
[20] B. J. Beaudry and K. A. Gschneidner, Jr., *Preparation and Basic Properties of the Rare Earth Metals*, in Handbook on the Physics and Chemistry of Rare Earths Vol. 1 (North-Holland, Amsterdam, 1978), Chap. 2.